Influence of CO2 on the NOx storage and reduction behavior of a NOx storage - reduction catalyst

Bouts, K.A.J.

Award date:
2006

Influence of CO_2 on the NO_x storage and reduction behavior of a NO_x storage – reduction catalyst

K.A.J. Bouts

March 2006

Graduation project

Coaches: Ir. C.M.L. Scholz
Dr. M.H.J.M. de Croon
Dr. Ir. J.H.B.J. Hoebink
Graduation Professor: Prof. Dr. Ir. J.C. Schouten

1. Summary

Stricter legislations on automotive emissions have led to the development of a NO_x storage reduction (NSR) catalyst for lean-burn gasoline and diesel engines. These engines operate under oxygen rich conditions, which make three-way catalysts, used in conventional gasoline driven engines, unsuited for use. The NSR catalyst is one of the most promising technologies to overcome this problem. During lean conditions, the catalyst (Pt-Ba-γ-Al_2O_3) stores NO_x as nitrates on barium. After a certain period the catalyst is filled with NO_x and regeneration is necessary. The operation is switched to oxygen poor conditions, by injecting extra fuel. This causes release and reduction of the stored NO_x. For lean operation, different Ba species have been reported, BaO, $Ba(OH)_2$ and $BaCO_3$. These species show differences in reactivity towards NO_x storage: BaO>$Ba(OH)_2$>$BaCO_3$. Moreover, different $BaCO_3$ sites have been reported. First there are well dispersed Low Temperature (LT) $BaCO_3$ sites, which cannot be detected by XRD. Secondly, bulky like High Temperature (HT) $BaCO_3$ sites have been reported, which can be detected via XRD because of they are crystalline.

The aim of this project is to investigate the influence of CO_2 on the NO_x storage and reduction behavior of the NO_x storage-reduction (NSR) catalyst. Therefore, transient kinetic experiments were performed, making use of a catalytic fixed bed reactor. Two separate feed lines were used. One contained NO and O_2 as oxidant (lean phase), the second contained H_2 as reducing agent (rich phase). Both streams used He as carrier gas. The in and outlet gas mixtures were monitored with a mass spectrometer. Experiments with and without CO_2 in the feed were performed.

The experiments without CO_2 showed a change in activity of the catalyst at lean/rich cycling of 30 and 120 min respectively. An improvement was observed in the activity followed by decline, i.e. NO_x storage first increased, then decreased, due to exchange of $BaCO_3$ sites for $Ba(OH)_2$. Furthermore, during rich conditions the selectivity towards N_2 production decreased. BET surface area, pore volume and Pt dispersion were measured which showed a 40 % decrease compared to a pretreated catalyst. XRD measurements showed formation of $Ba(NO_3)_2$ indicating HT participation. Experiments with CO_2 in the reactor feed at lean/rich cycling of 9 and 15 hrs respectively showed no activity or selectivity change. Physical properties were measured and showed no deviations compared to a pretreated catalyst. XRD measurement showed no $Ba(NO_3)_2$, which implies that HT sites have not participated in the storage process.

Furthermore, lean/rich cycling of 9 and 15 hrs respectively were done at different temperatures. The results showed differences in NO breakthrough time, in the lean phase. The rich phase shows at lower temperature a decline in the selectivity towards N_2 production. Moreover, NO production was higher at elevated temperatures, in the rich phase. At all temperatures, ultimately 30 % Ba utilization was reached.. With different lean/rich timing in the order of minutes, NO_x breakthrough was observed earlier for longer rich timing, during lean operation. During rich operation, the same observation as during lean operation was observed for the N_2 production timing.

Mechanistic studies showed that several routes towards NO_x storage take place. Moreover, nitrites are formed which can be further oxidized by NO_2 to nitrates. Also the rich phase showed that mostly nitrates have been formed during lean operation. The acquired data should lead to verification of a kinetic model describing the NO_x storage and reduction behavior.

2. Table of contents

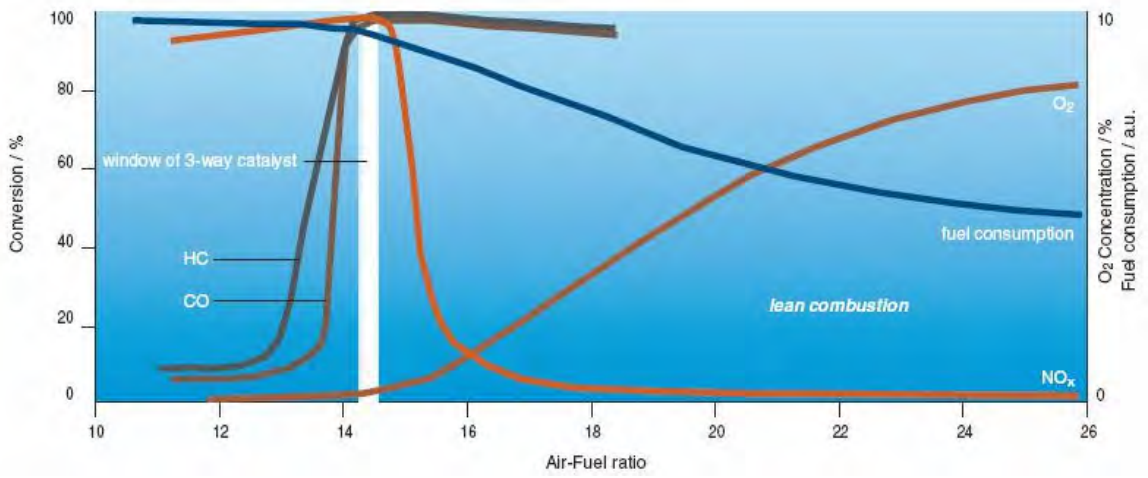

Figure 1: *Fuel consumption and TWC performance as a function of air to fuel ratio [1].*

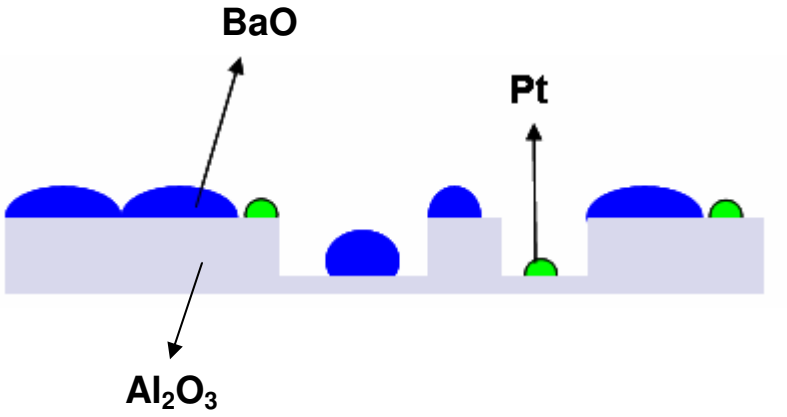

Figure 2: *Schematic overview of a NO_x storage reduction catalyst.*

3. Introduction

3.1. General description

The environment is an important issue in today's society. People have come to grip with the idea that the air pollution that is being produced by industry and the cars we drive, must be dealt with. In 1970 the Clean Air act in the USA set the standard for automotive emissions. This led to the development of the modern three-way catalyst (TWC). The TWC is able to reduce the emissions of hazardous components such as CO, C_xH_y and NO_x. This catalyst was incorporated in petrol driven cars. From January 1st 1993 all new petrol driven cars in the Netherlands are obligated to have such a TWC on board in order to comply with emission standards. The TWC consists of a γ-Al_2O_3 support with Pt particles and small amounts of other metals, deposited on the surface. On these metal sites, the mentioned components are converted into less polluting ones. Important in the operation of the TWC is the air to fuel ratio (Figure 1). The typical operating window for the TWC is at an air to fuel ratio of 14.5 which corresponds to the combustion of petrol driven engines. But because of their high fuel consumption, diesel and lean-burn engines have become more and more interesting. For these engines a catalyst was not necessary in the early 1990's because they still conformed to emission legislations. However, with more rigid legislations, these engines cannot escape the use of a catalyst anymore.

The diesel and lean-burn engines contain an excess amount of oxygen in their exhaust. As a result the engine is operated outside the operating window of the TWC, leading to a NO_x conversion of almost 0 (Figure 1). One of the most suitable technologies to overcome this problem is the NO_x trap, designed by Toyota Motor Company [1]. With this technology a component is added to the TWC, which functions as a trap. Suitable components are earth alkaline metal oxides such as BaO, of which a large amount is deposited on the TWC (Figure 2), i.e. on Pt-γ-Al_2O_3. These catalysts are called NO_x storage reduction (NSR) catalysts

The operation of a NSR catalyst consists of two parts. First the storage phase or lean phase takes place, followed by the reducing or rich phase. Lean operation takes place at high air to fuel ratio (Figure 1), i.e. oxygen rich conditions, whereas rich operation takes place in the operating window of the TWC, i.e. oxygen poor conditions. A schematic overview of the lean combustion process is depicted in Figure 3. During lean combustion, the catalyst starts to store NO_x (the black particles). As the operating time increases, the catalyst bed gets saturated with NO_x, approaching inlet concentration. Now the engine will be set to operate under rich conditions and the NO_x is reduced, thus "cleaning" the catalyst.

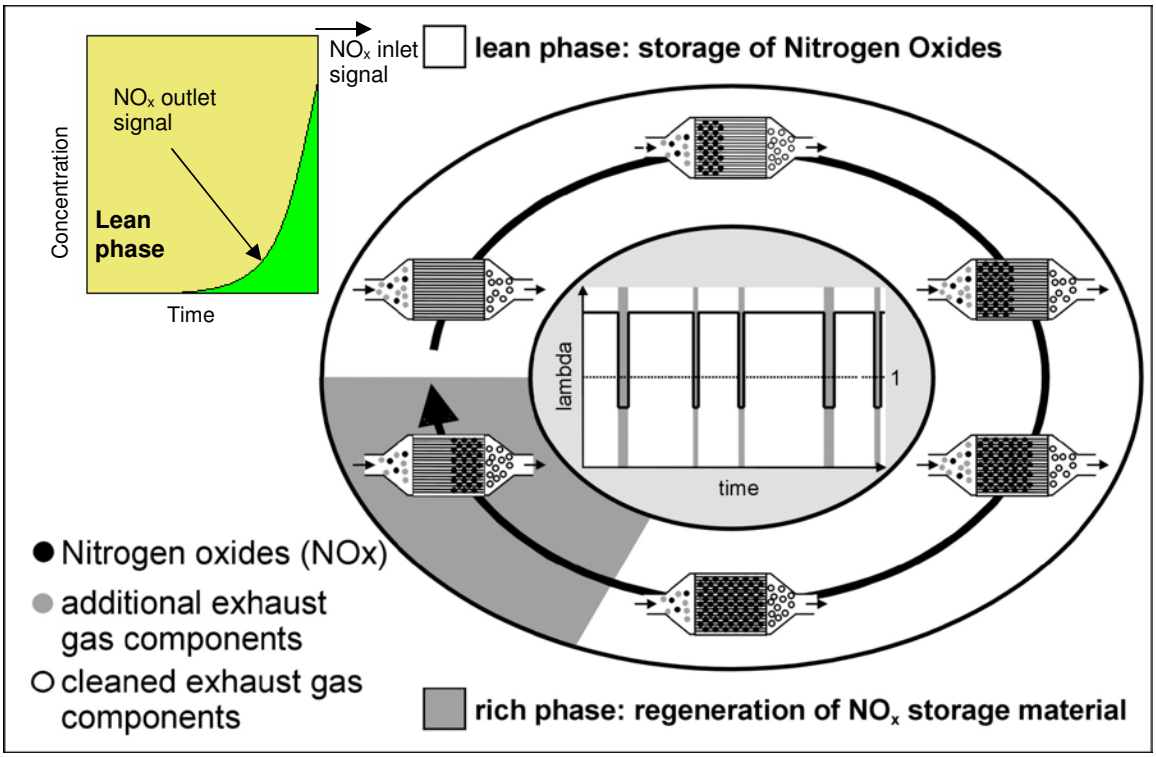

Figure 3: *Schematic overview of the operating mode of a NSR catalyst [21].*

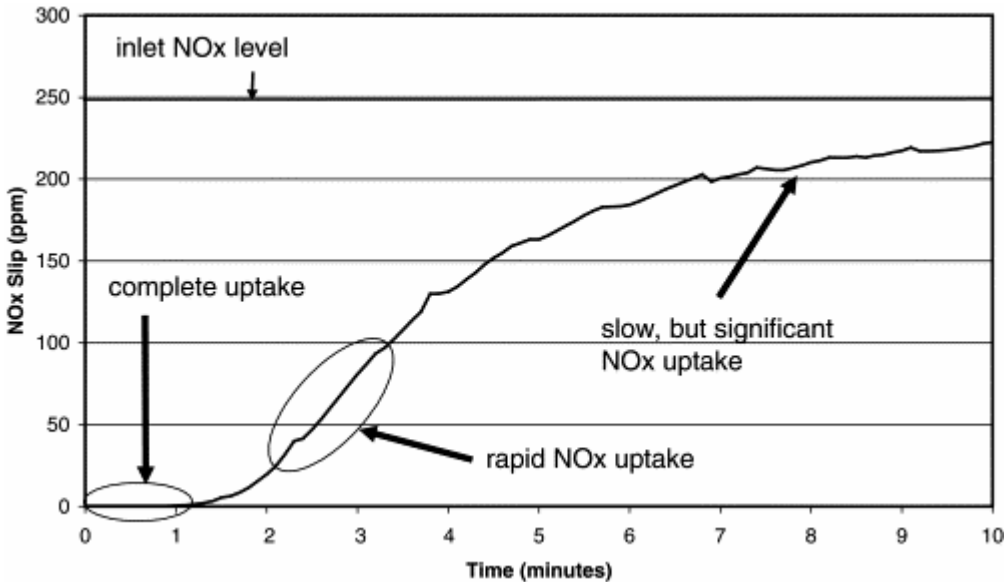

Figure 4: *NO_x storage characteristics: Complete uptake followed by rapid NO_x uptake, leading to slow NO_x uptake [10].*

3.2. The NO_x storage – reduction catalyst

3.2.1. Lean phase

During lean operation NO_x storage takes place. This storage process can generally be divided into several pathways. One of the most important steps is the NO oxidation into NO_2 on Pt, represented in Equation 1 [3,17,18].

$$NO + ½\,O_2 \xleftrightarrow{Pt} NO_2 \qquad \text{(Eq. 1)}$$

NO_2 can subsequently be stored through the disproportionation mechanism (DPM) [3,4,12], resulting in NO release:

$$3\,NO_2 + BaO \rightarrow Ba(NO_3)_2 + NO \qquad \text{(Eq. 2)}$$

It is furthermore possible to have storage of NO_2 directly into nitrates, without NO formation, as shown in Equation 6 [3,17]. It is also reported in literature that NO can be stored into nitrites as described in Equation 4 [16].

$$2\,NO_2 + BaO + ½\,O_2 \rightarrow Ba(NO_3)_2 \qquad \text{(Eq. 3)}$$

$$2\,NO + BaO + ½\,O_2 \rightarrow Ba(NO_2)_2 \qquad \text{(Eq. 4)}$$

$Ba(NO_2)_2$ formed in Equation 4 can further be oxidized to form nitrates by reaction with NO_2 [3, 17]:

$$Ba(NO_2)_2 + 2\,NO_2 \rightarrow Ba(NO_3)_2 + 2\,NO \qquad \text{(Eq. 5)}$$

Epling et al. described the NO_x storage process divided into three stages [12], these are shown in Figure 4. First there is complete NO_x storage. Secondly one can see rapid NO_x uptake and an increase in the NO_x output signal. Finally there is a slow but measurable NO_x uptake. This rate does not quickly reach zero. Epling et al. mention that these stages can be associated with multiple storage sites involved in the storage. Depending on experimental conditions Ba will be present as BaO, $Ba(OH)_2$ and $BaCO_3$. Equations 2, 3 and 4 can take place on $Ba(OH)_2$ and $BaCO_3$ as well, resulting in H_2O and CO_2 formation respectively. In literature differences in reactivity are described for these components, specifically BaO > $Ba(OH)_2$ > $BaCO_3$ [5]. Mahzoul et al. [2] described a difference in Ba sites with respect to their geometry. They argue that Ba sites close to Pt, where NO is oxidized, are able to store oxidized NO_x, whereas Ba sites further away from the oxidizing Pt sites are less reactive towards storage. Besides the different Ba sites, also a difference in $BaCO_3$ sites is described in literature. Recent work of Piacentini et al. [10,11] shows that two $BaCO_3$ sites can be distinguished. They subjected calcined catalyst samples to temperature programmed desorption (TPD) resulting in a small peak around 700 ^oC. The sites connected to this TPD signal, are called Low Temperature $BaCO_3$ sites (LT), which are finely dispersed particles of $BaCO_3$ on the γ-Al_2O_3 surface. These particles are amorphous and can therefore not be detected via X-ray diffraction (XRD). A second peak was observed at 1000 ^oC, which they denote as High Temperature $BaCO_3$ sites (HT). These sites are bulky like sites or clusters that are crystalline and can hence be detected via XRD measurements. This provides the possibility to discriminate between the different sites that participate in the storage process. Chen et al. [19] deposited $Ba(NO_3)_2$ on Pt-γ-Al_2O_3 and performed thermal gravimetric analysis which

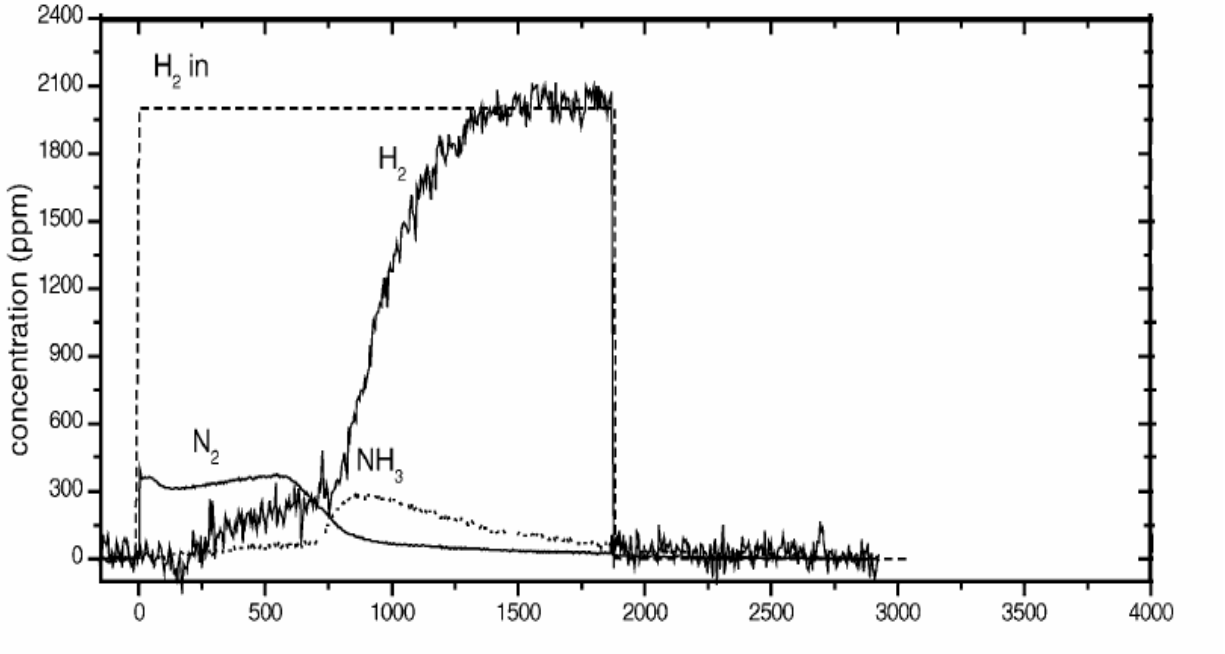

Figure 5: *N_2, NH_3 H_2 outlet and H_2 inlet concentrations vs. time upon H_2 addition on Pt-Ba(x)/γ-Al_2O_3 at 350 ^oC. Ba loading is 23 % [7].*

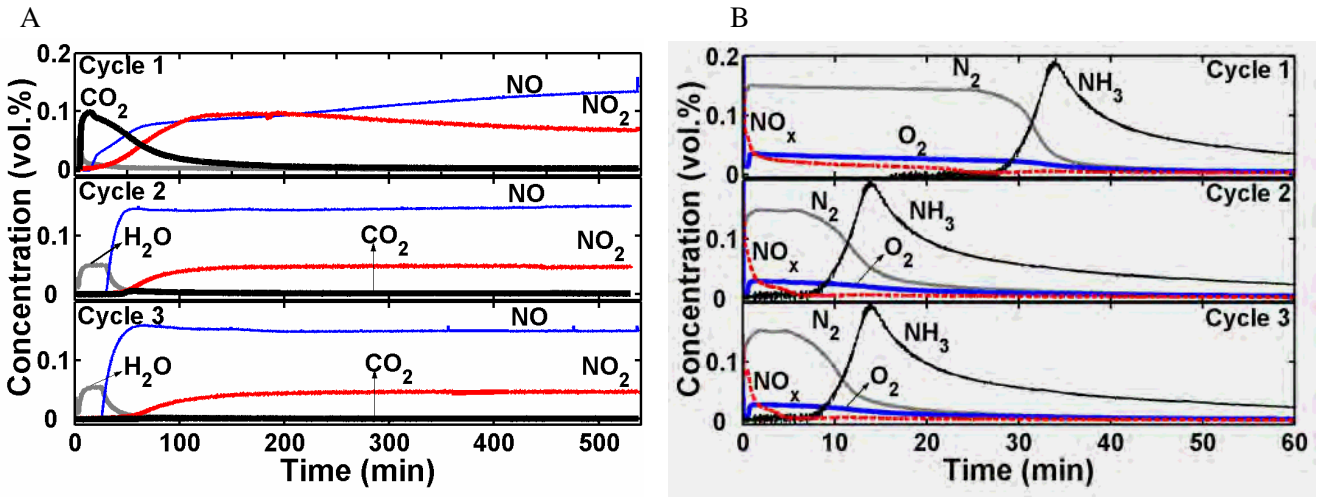

Figure 6: *a) Lean outlet concentrations of NO, NO_2, CO_2 and H_2O signal during three subsequent cycles, starting with a pretreated catalyst. Lean phase: 0.2 vol. % NO, 4 vol. % O_2 and 1 vol. % Ar, 9 h. b) Rich outlet concentrations of NO_x, N_2, O_2 and H_2O during three subsequent cycles. Rich phase: 0.8 vol. % H_2 and 1 vol. % Ar in He, 15 h. T= 643 K. Only the first 60 min of the rich phase are shown [13].*

showed three peaks: the first is observed below 100°C, which is weight loss due to physically adsorbed H_2O. The second one is observed around 400°C which are LT sites. The third one is observed above 550 °C which can be ascribed to bulk $Ba(NO_3)_2$ or HT sites.

3.2.2. Rich phase

During rich operation, i.e. oxygen poor operation, the stored nitrates and nitrites are released and subsequently reduced on Pt to N_2 [12]. Several reducing agents are used in literature, such as CO, C_3H_6 and H_2; all of them are present in real life exhaust gases. In this research H_2 is chosen to be the reducing agent. The reactions towards N_2 production that can take place are depicted in Equations 6 and 7.

$$Ba(NO_3)_2 + 5\ H_2 \xrightarrow{Pt} Ba(OH)_2 + N_2 + 4\,H_2O \qquad \text{(Eq. 6)}$$

$$Ba(NO_2)_2 + 3\ H_2 \xrightarrow{Pt} Ba(OH)_2 + N_2 + 2\,H_2O \qquad \text{(Eq. 7)}$$

The N_2 production is observed immediately after switching to rich conditions (Figure 5). Besides N_2 formation, NO_x release is observed during the rich phase [5,14]. The amount of NO released however, is quite small. Castoldi et al. observed during NO_x release and reduction, at lower temperatures up to 300°C, NH_3 production [7]. NH_3 production takes place via Equation 8.

$$Ba(NO_3)_2 + 8\,H_2 \xrightarrow{Pt} 2\,NH_3 + Ba(OH)_2 + 4\,H_2O \qquad \text{(Eq. 8)}$$

NH_3 production is only observed after N_2 production has decreased to zero (Figure 5). With H_2 as the reducing agent, the NO_x reduction is highly selective towards N_2 production [5]. This selectivity can be calculated as presented in Equation 9, the reduction efficiency.

$$\text{Reduction efficiency} = \frac{2*[N_2]}{2*[N_2]+[NO_x]+[NH_3]} \qquad \text{(Eq. 9)}$$

3.2.3. Catalyst activity

Recent work has been done on lean/rich cycling in the order of hours [13]. Figure 6 represents the experiments performed in this work. The first lean phase shows NO breakthrough after 14.1 min. NO_2 evolves after 16.5 min and shows a maximum after breakthrough. This indicates a change in the NO oxidation efficiency in time during NO_x storage. During the corresponding rich cycle, not all of the Ba that has participated in the storage was regenerated (Table 1), even after a 15 hrs rich phase. The subsequent lean phase shows an increase in breakthrough time for NO and NO_2. During rich again not all of the Ba sites were regenerated. In addition an increase in NH_3 production was observed indicating that the selectivity towards N_2 production decreased. The lean phase of the third cycle shows a decrease in breakthrough timing for NO and NO_2. The Ba participation is 60%. The decrease in NO oxidation efficiency and incomplete regeneration of

Table 1: *Barium utilization for lean and rich phases. Lean phase: 0.2 vol. % NO, 4 vol. % O_2 and 1vol. % Ar in He, 9 hrs. Rich phase: 0.8 vol. % H_2 and 1 vol. % Ar in He, 15 hrs. T=643 K. Pretreated catalyst was used. See also Figure 6 [13].*

Cycle no	**1**	**2**	**3**
Lean phase			
% Ba active	93	71	60
% Ba active as BaO	6	37	36
% Ba active as $Ba(OH)_2$	11	26	24
% Ba active as $BaCO_3$	76	8	-
Rich phase			
% Ba reduced	79	60	59

stored NO_x during rich phase operations were also observed when performing the same experiment at different temperatures. These observations could be due to masking of Pt sites by barium. During the NO_x storage, $Ba(NO_3)_2$ is formed which has twice the molar volume of $BaCO_3$ resulting in coverage of Pt sites or blocking of catalyst pores. Therefore the BET surface area and Pt dispersion were measured (Table 2), which both showed a large decrease compared to a pretreated catalyst. According to these observations, Pt is essential for NO oxidation/reduction as well as for $Ba(NO_3)_2$ decomposition [4,13]

Table 2: *BET surface area, pore volume and Pt dispersion. The data shown for the catalyst after a lean phase and a rich phase are data measured after the catalyst had reached the cyclic steady state [13].*

	BET (m^2/g)	**Pore volume (cm^3/g)**	**Pt dispersion (%)**
Pretreated catalyst	70	0.22	20
After lean phase	43	0.15	11
After rich phase	45	0.18	11

3.2.4. Influence of CO_2

Although CO_2 is present in real exhaust gas, not much research has been done on the influence of CO_2 on the NO_x storage reduction mechanism. CO_2 has a negative effect on the amount of NO_x stored [5,6,12]. Lietti et al. found that this negative effect is most significant at low temperatures [6]. Epling et al. however, found that CO_2 has a large inhibiting effect at especially high temperatures [15]. Further Epling et al. found, although CO_2 significantly influences the initial interval of NO_x trapping, CO_2 has a smaller influence on the capture efficiency after NO_x starts breaking through. The significant decrease of NO_x storage in the presence of CO_2 suggests there is a competitive storage between NO_x and CO_2 [3,22]. Rodrigues et al. concluded furthermore, that the well dispersed $BaCO_3$ sites form probably the NO_x trapping sites [22].

By introducing CO_2 to the helium flow a significant increase in the NO_x release rate is observed [14]. This observation has also been made by Amberntsson et al. who explained this on thermodynamic grounds [20]. For the reduction, with H_2, CO_2 has only an inhibiting effect on the reduction towards N_2 at higher temperatures [5,15]. Furthermore, Lietti et al. [5] found that during reduction with H_2 the Ba sites are transformed into BaO and $Ba(OH)_2$, while in the

presence of CO_2 all the Ba sites are transformed into $BaCO_3$. With the introduction of CO_2 in the rich phase the reversed water gas shift reaction will take place as described in Equation 10 [12].

$$CO_2 + H_2 \rightarrow CO + H_2O \qquad \text{(Eq. 10)}$$

3.3. Project outline

This study is part of a major STW Ph.D. project entitled: "A model-based controller for diesel and lean burn engines, to optimize both emissions and fuel consumption."

In order to come up with a proper model, a detailed understanding of the kinetics taking place is important. The kinetic model should be able to describe the lean/rich cycling operation. This should be able to predict the lean/rich switching times needed to have optimal storage and reduction conversions. Experimental data with different conditions are of course required to verify the described kinetic model

As described in section 3.2.3. Catalyst activity, the catalyst performance changes at lean/rich cycling of 9 and 15 hrs respectively. With shorter cycling times it could well be that these changes are not achieved. Therefore, lean/rich cycling experiments in the order of minutes will be discussed to trace if this change can also be observed when there is a much shorter lean/rich exposure.

1. Investigation of catalyst activity at lean/rich cycling times in the order of minutes.

In the automotive exhaust CO_2 is present in a large quantity. Therefore, it is useful to investigate the influence it has on the storage and reduction process of the NSR catalyst. Attention will be given to the activity change of the catalyst, since it changes when no CO_2 is present.

2. Investigation of catalyst activity at lean/rich cycling times in the order of hours, with CO_2 in lean and rich feed.

These experiments will be performed at different temperatures and lean/rich timing.

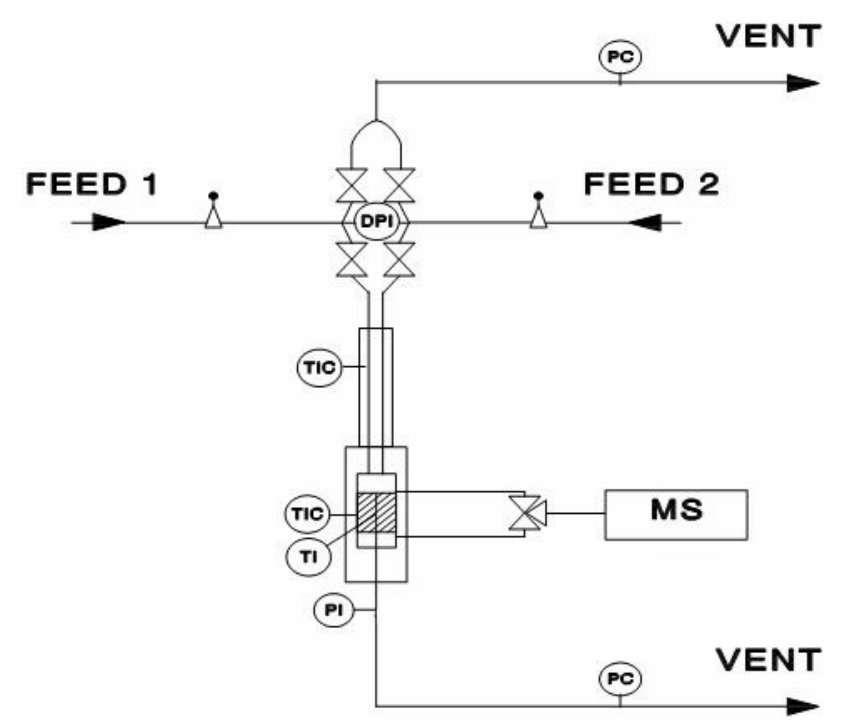

Figure 7: *Schematic overview of the reactor set-up.*

4. Experimental set-up

The experimental data are obtained by performing feed cycling experiments with a lean (oxygen rich) and rich feed (fuel rich) over a catalytic fixed bed. The experimental set-up consists of a reactor system with two different feed lines and an analysis section. A schematic overview is shown in Figure 7.

4.1. Feed section

The inlet consists of two separate feed lines, depicted in Figure 7 as feed 1 and 2. The composition of feed 1 and 2 represent the composition of the rich and lean phase, respectively. Each feed line has its own set of mass flow controllers. In this way, two different gas compositions can be created independently. The stream which is not fed to the reactor is directed to the ventilation in order to avoid pressure changes after the feed switches, e.g. if feed 1 is led over the reactor, feed 2 is directed to the ventilation.

When switching between two reactor feeds, with different composition, the overlap between the feeds during the switch should be minimal in order to avoid mixing of feeds as much as possible. For this reason, fast magnetic valves, which open and close in a couple of milliseconds, are used for switching the feed between the reactor and the ventilation. Upon switching between feed A and B it is necessary to have as little overshoot as possible, i.e. on or of switching should result in a block shaped signal. This can be controlled by two back pressure controllers placed in the feed lines.

The feed section is provided with a pre-heater making sure the desired reactor temperature is reached. This temperature is measured with a thermocouple placed in the pre-heated section just above the reactor. Furthermore, the gas lines are heated throughout the system.

4.2. Reactor section

The reactor is a fixed bed reactor made of titanium. It has a length of 15 mm and a diameter of 14 mm. The catalyst bed consists of 1.9 g. Pt-Ba-Al_2O_3 in powder form, with a particle size of 212-250 μm, as provided by Engelhard, and is retained by two sintered plates. The reactor tube is heated by a coil wrapped around the reactor jacket. The temperature is controlled at three sections on the outside of the reactor wall. The temperature inside the catalyst bed can be monitored with three thermocouples placed in different axial positions: in the center of the reactor and 3 mm above and below the center, to check isothermal conditions. The radial temperature profiles are monitored via a thermocouple placed on the outside of the reactor wall. This thermocouple is used as input for a PID controller, which sets the reactor temperature.

4.3. Analysis section

The online measuring takes place via an ESS quadrupole mass spectrometer (MS). Capillary inlets are placed right above and below the reactor bed. In order to have an internal standard during experiments and calibration, a fixed amount of argon is fed. Furthermore, argon can be used to compensate for any intensity loss of the mass spectrometer. Appendix 2 shows how this compensation is achieved.

The gas analysis were performed on m/e 2 (H_2), 14 (N_2, NO, NO_2), 17 (NH_3), 18 (H_2O), 28 (N_2 + CO_2 + CO), 30 (NO + NO_2), 32 (O_2), 40 (Ar), 44 (CO_2) and 46 (NO_2, CO_2). For the overlap of CO_2, overlap on m/e 14, 28 and 30, corrections are performed.

4.4. Characterization methods

Besides monitoring reaction conditions and composition changes, the physical changes in the catalyst have been investigated. The following methods have been used:

- Brunauer Emmett Teller adsorption measurements. The surface area per gram catalyst can be measured, including the pore volume of the catalyst. These measurements were conducted with the use of a Micromeritics Tristar instrument, at -196 ^{o}C, with N_2 as adsorbent.
- Pt-dispersion measurements. This chemisorption is conducted at 25 ^{o}C using a Micromeritics ASAP 2000 and 2020 instrument. This measurement is conducted on pretreated catalyst samples and catalyst samples used in lean/rich cycling experiments.
- X-ray diffraction. This method is used to investigate the composition of the catalyst. The powder XRD measurements were performed on a Rigaku Geigerflex diffractometer. The spectra were recorded in the range $15^{o} < 2\theta < 75^{o}$ using CU-Kα radiation.
- Thermal gravimetric analysis (TGA). Via this method desorption of the gaseous products from the surface of solids has been studied in vacuum under the desired temperature profile. The gases released are monitored by a MS. The temperature interval was set at 25-1100 °C, with a temperature ramp of 10 ^{o}C/min. The vacuum reaches a pressure up to 10^{-6} bar. The amount of sample required for interpretable results is 50 to 100 mg. Via this method, the temperature of desorption of certain compounds, the relative strength of the active sites and their relative amount can be measured. In this study this was done for CO_2.

4.5. Experimental conditions

4.5.1. Catalyst pretreatment

In order to be able to perform reproducible kinetic experiments, the catalyst must be conditioned properly before starting experiments. The experimental sequence performed in pre-treating the catalyst is depicted in Table 3.

Table 3: *Experimental sequence for the pretreatment of the catalyst.*

Conditions / Pretreatment phase	Temp. (^oC)	He (v%)	O_2 (v%)	H_2 (v%)	Duration (min)
Heating	25 → 500	100	0	0	--
Oxidation	500	99	1	0	60
Purge	500	100	0	0	30
Reduction	500	98	0	2	120
Cooling	500 → 25	100	0	0	--

4.5.2. Experimental procedure

As mentioned in section 3.3. Project aim, 2 different types of experiments have been conducted: Experiments with and without CO_2 in the feed. The experiments without CO_2 have been performed with lean/rich cycling in the order of minutes. Furthermore, experiments with lean/rich cycling in the order of hours and CO_2 in the feed have been conducted. The experiments with CO_2 in the feed, have been differentiated in temperature and lean/rich cycle times. Finally experiments with fast lean/rich cycling have been conducted which come close to real time operating conditions. The conditions used for these experiments are depicted in Table 4.

Table 4: *Experimental sequence, with lean/rich timing and temperature.*

	Lean (min)	Rich (min)	Temp. (^oC)	CO_2	Comment
1	15	60	300	No	
2	30	120	300	No	
3	540	900	370	Yes	
4	540	900	300	Yes	
5	540	900	240	Yes	
6	30	120	300	Yes	
7	30	50	300	Yes	
8	30	120	300	Yes	1.2 v% H_2
9	30	900	300	Yes	
10	4	1	300	Yes	
11	4	1	370	Yes	
12	4	1	240	Yes	

The lean and rich feed concentrations expressed in v% are depicted in Table 5; He was used as carrier gas.

Table 5: *Lean and rich feed concentrations in v%,, used in the experiments described in Table 4.*

	NO	O_2	H_2	Ar	(CO_2)
Lean	0.2	4	0	1	10
Rich	0	0	0.8	1	10

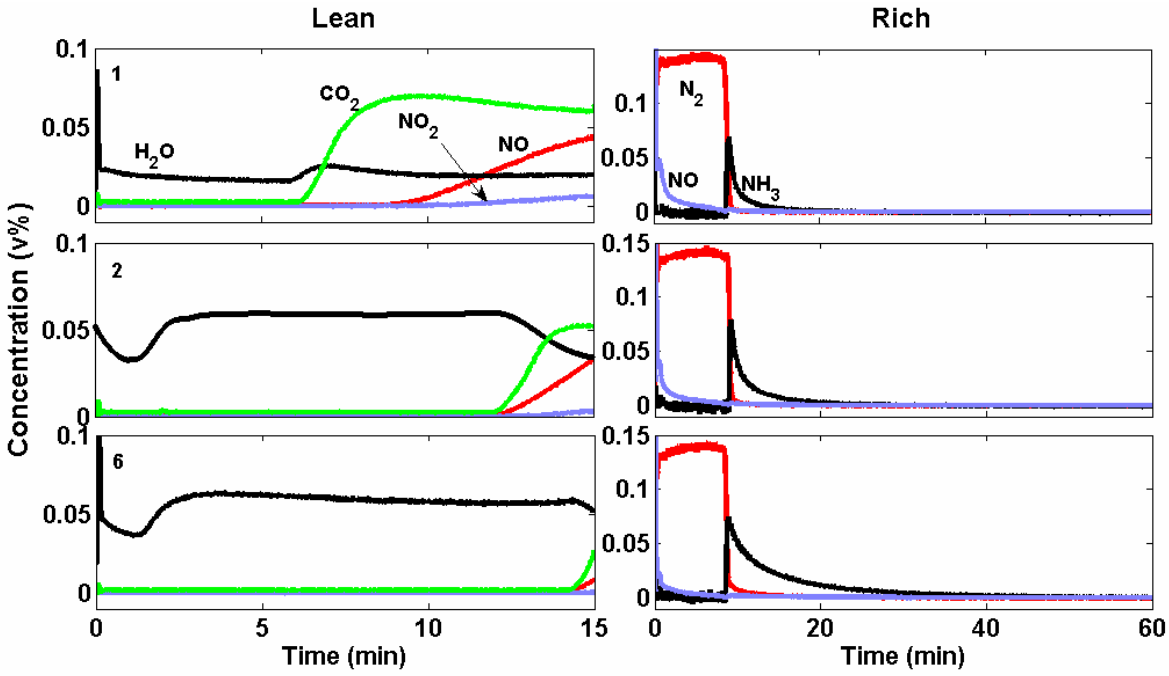

Figure 8: *Results for lean/rich cycling of 15 and 60 min respectively, without CO_2,in the feed. T=300 °C. Cycle nrs. 1, 2, 6 are shown. Lean phase: 0.2 v% NO, 4 v% O_2, 1 v% Ar. Rich phase: 0.8 v% H_2, 1 v% Ar. He as carrier gas was used.*

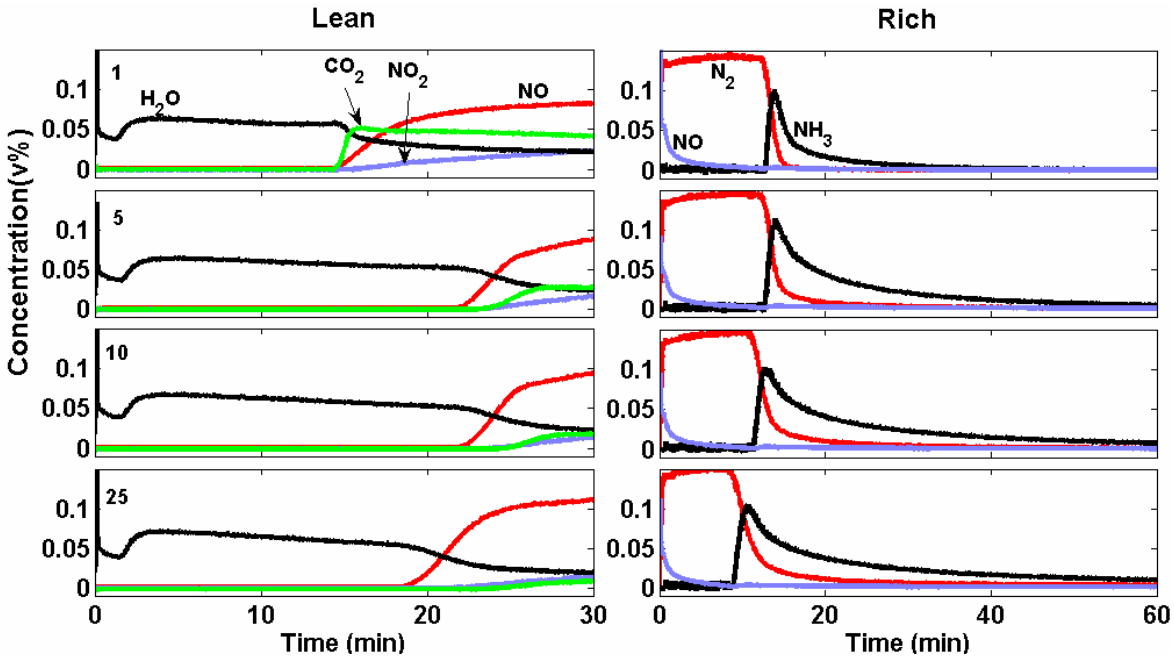

Figure 9: *Results for lean/rich cycling of 30 and 120 min respectively, without CO_2,in the feed. T=300 °C. Cycle nrs. 1, 5, 10 and 25 are shown. Lean phase: 0.2 v% NO, 4 v% O_2, 1 v% Ar. Rich phase: 0.8 v% H_2, 1 v% Ar. He as carrier gas was used.*

5. Results

5.1. Activity change

Figure 8 represents the results for the experiment with lean/rich cycling of 15 and 60 min respectively, in terms of concentration in v% as a function of time in minutes. Cycles 1, 2 and 6 are shown.

From the start of the first lean phase, H_2O evolution is seen. This indicates $Ba(OH)_2$ participation in the storage process. After approximately 6 min CO_2 evolves. This evolution indicates participation of $BaCO_3$ in the storage process. A reason for this delay can be the lower reactivity towards NO_x storage than BaO and $Ba(OH)_2$ [5]. Breakthrough of NO is observed after 8.5 minutes of lean operation and NO_2 evolution is observed about 1 min later. The involvement in storage of the different Ba containing species with respect to the total amount of Ba present is presented in Table 6. The $Ba(OH)_2$ participation is 3.1 %, $BaCO_3$ participation in the storage is 5.6 % and BaO participates for 6.3 %. The total amount of NO_x that is stored corresponds to 15 % Ba utilization, on the basis of 2 moles of NO_x being stored on 1 mole of Ba. Furthermore, in the calculations NO_x is only stored on Ba sites.

The subsequent rich phase shows immediate N_2 production and NO release. The N_2 production almost immediately reaches a level of 0.14 v% and remains constant for about 8.5 min after which it rapidly decreases to zero. NH_3 formation is observed right after this rapid decrease of N_2. The mentioned NO desorption decreases gradually to zero. The total amount of reduced $Ba(NO_3)_2$ is 14.3 %. Reduction of $Ba(NO_3)_2$ to N_2 is 13 %, with 1 mole of N_2 corresponding to 1 mole $Ba(NO_3)_2$. NO release is responsible for 0.7 %, with 2 moles of NO corresponding to 1 mole $Ba(NO_3)_2$,. The NH_3 formation corresponds to 0.6 % $Ba(NO_3)_2$ released. The reduction efficiency is equal to 86.7 %.

Table 6: *Quantitative results, lean/rich cycling of 15 and 60 min respectively, T=300 °C and no CO_2 in the feed.*

Cycle nr.	**1**	**2**	**6**
Lean			
$Ba(OH)_2$ %	3.1	8.4	9
$BaCO_3$ %	5.6	1.4	0.4
BaO %	6.3	5.8	6.4
Ba% total	15	15.6	15.8
Breakthrough time NO (s)	510	710	840
Rich			
Ba% total	14.3	15.1	16.3
Ba% N_2	13	13.5	13.3
Ba% NO_x	0.7	0.7	0.5
Ba% NH_3	0.6	0.9	2.5
Reduction efficiency (%)	86.7	89.4	81.6

Switching to cycle number 2, an improvement of the catalyst's performance in the lean phase is observed. This is represented by an increased NO breakthrough time, resulting in a higher NO_x storage. Furthermore CO_2 breaks through later in this cycle, which is an indication that there are

less $BaCO_3$ sites available for storage. During the previous rich phase, $Ba(NO_3)_2$ was exchanged for $Ba(OH)_2$ and not for $BaCO_3$ because CO_2 was absent in the feed. With more $BaCO_3$ being exchanged for $Ba(OH)_2$ the storage increases. This is an indication for a difference in reactivity in favor of $Ba(OH)_2$. The corresponding rich phase shows that the amount of stored NO_x, is released and/or reduced. However, the amount of NH_3 that is formed is higher than for the first cycle. This indicates an unwanted loss in selectivity towards N_2 formation of the catalyst during rich operation. Cycle nr. 6 shows again an improvement of the catalyst's performance in the way described for cycle 2. Moreover, the rich phase shows complete regeneration and a decrease in selectivity.

Because there is almost no CO_2 in the outlet signal, a switch is made towards lean/rich cycling experiments of 30 and 120 min respectively. The results are depicted in Figure 9 with concentrations in v% as a function of time in minutes. Cycles 1, 5, 10 and 25 are shown.

Starting from cycle nr.1 we can observe immediate H_2O formation. After 14.3 min we can see $BaCO_3$ participating in the storage process. NO breaks through slowly at the same moment as CO_2, followed by NO_2 at approximately 14.5 min. The total amount of NO_x that is stored is 25.5 % (Table 7). The amount of NO_x stored on $Ba(OH)_2$ sites is 13.5 %, $BaCO_3$ involvement is 7.3 %. The remaining 4.7 % accounts for the BaO involvement. The catalyst's performance is still improving as can be seen from the breakthrough timing of NO_x.

Table 7: *Quantitative results, lean/rich cycling of 30 and 120 min respectively, T=300 °C, no CO_2 was present in the feed.*

Cycle nr.	**1**	**5**	**10**	**25**
Lean				
$Ba(OH)_2$ %	13.5	15.9	16.4	15.6
$BaCO_3$ %	7.3	1.0	0.4	0.5
BaO %	4.7	11.9	11.9	10.6
Ba % total	25.5	28.8	28.7	26.7
Breakthrough time (s)	860	1260	1260	1070
Rich				
Ba% total	23.9	27.4	28.2	27
Ba% N_2	20.5	20.5	19.8	17.2
Ba% NO_x	1.2	0.9	0.9	0.9
Ba% NH_3	2.2	6.0	7.5	8.9
Reduction efficiency (%)	85.8	74.8	70.2	63.7

The subsequent rich phase shows immediate N_2 formation and NO release. The N_2 formation reaches a level of 0.14 v% and stays constant for 12.5 min, after which it rapidly decreases. The NO release decreases towards zero immediately after the start. NH_3 formation is again observed after the decrease in N_2 concentration and decline of NO. The peak is about 0.1 v% and decreases slowly towards zero. The amount of N_2 that is formed is 20.5 %, NO_x release is 1.2 % and NH_3 accounts for 2.22 % of the reduced Ba. The reduction efficiency is 85.8 %.

For cycles 2-10 during lean operations, an improvement of the catalyst's storage performance is observed, indicated by an increase in the NO breakthrough time. Moreover a decrease in $BaCO_3$ participation is observed which can be ascribed to the exchange of $BaCO_3$ for $Ba(OH)_2$. The rich phase shows similar results for N_2 and NH_3 production compared to the previous experiment,

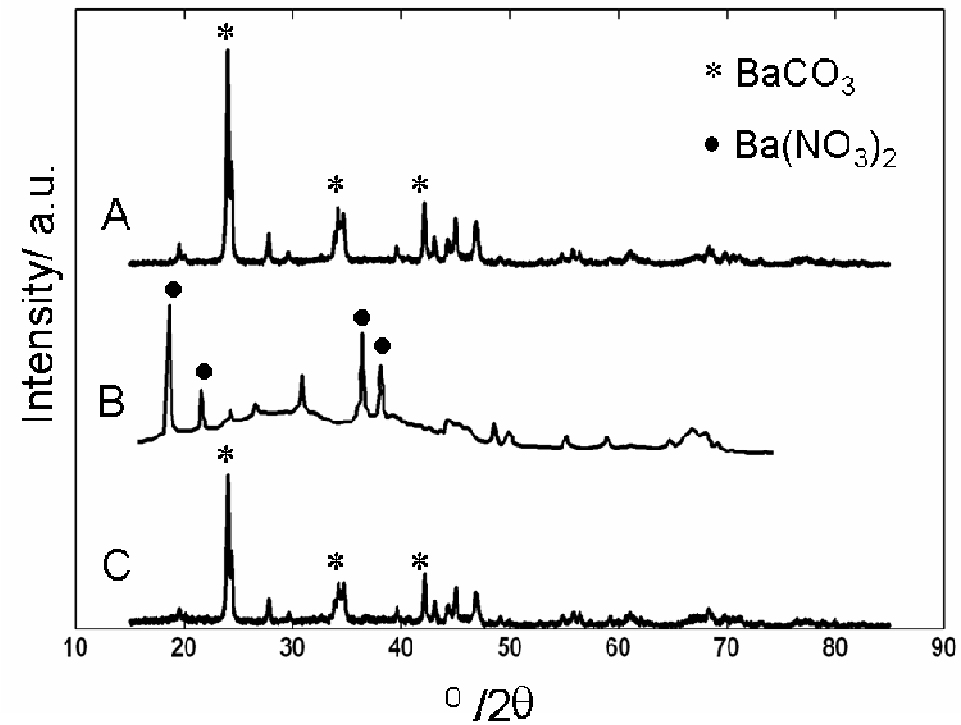

Figure 10: *XRD patterns of a fresh catalyst (A), after lean/rich cycling without CO2, ending with lean exposure (B), after lean/rich cycling with CO2, ending with lean exposure (C).*

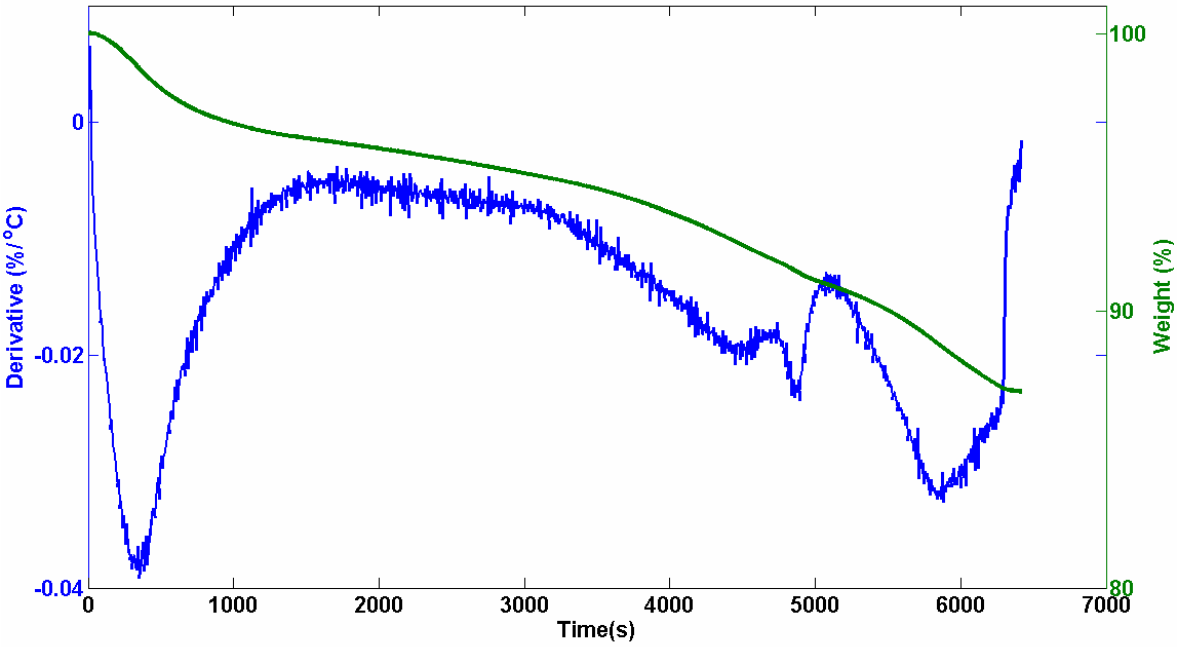

Figure 11: *TG-DTG curve with TGA heating rate of 10 °C/min for thermal decomposition of Pt-Ba-γ-Al_2O_3 The TGA heating rate was set at 10 °C/min, starting from room temperature.*

immediate N_2 formation and an increase in NH_3 production. The released/reduced amount is however not same as the amount stored. When observing cycle nr. 25 deterioration of storage is observed. The amount stored however, is now again completely released and reduced. The decline in storage could be due to coverage of Pt sites by Ba. The stored $Ba(NO_3)_2$ has twice the molar volume of $BaCO_3$, coverage can thus be extended and blocking of catalyst pores can occur. The blocking of pores results in a decrease in pore volume and BET surface. Therefore a BET measurement was performed. The results are depicted in Table 8, where a comparison is made with a fresh pretreated catalyst. Indeed, the adsorption measurement shows a decrease in surface area and pore volume. Also, the Pt dispersion has decreased. Furthermore, an XRD measurement was performed to see which type of $BaCO_3$ sites participate in the storage process. The result is shown in Figure 10(B). Here $Ba(NO_3)_2$ is observed, implying that bulky sites have participated in the process which correspond to HT sites. This however, does not exclude the possibility that LT sites have participated in the storage process.

Table 8: *BET, Pore volume and Pt dispersion for Pt-Ba-γ-Al_2O_3, for a fresh catalyst, after lean exposure and after rich exposure.*

Conditions	**BET (m^2/g)**	**Pore volume (cm^3/g)**	**Pt – dispersion (%)**
Pretreated catalyst	74	0.22	20
Without CO2, after lean	42	0.16	11
Without CO2, after rich	47	0.18	11

5.2. Characterization of $BaCO_3$

In order to quantify the $BaCO_3$ sites present in the catalyst sample, a TG/DTG experiment has been performed on a fresh sample. The TGA heating rate was set at 10 ^oC/min. The results are shown in Figure 11, with weight loss % as a function of temperature in degrees Celsius. The TGA analysis shows 4 peaks. The first peak is observed at 100 ^oC and can be ascribed to H_2O desorbing from the catalyst. The catalyst has been exposed to air for a long time resulting in the presence of H_2O. the second peak starts at approximately 600 ^oC and ends at 800 ^oC. It corresponds to findings of Piacentini et al. [10] who also found a CO_2 peak at this temperature and denounced it LT sites. Next a sharp peak is observed at 800 ^oC. The $BaCO_3$ sites that correspond with this peak are most probably also LT sites. Piacentini et al. describe BaO sites that can be converted into $BaCO_3$ when exposed to air for a considerable amount of time. They mention that the second peak can be ascribed to these sites. In this case, the catalyst has been exposed to air for several years. Thus these sites can probably be ascribed to what has been reported by Piacentini. Finally a peak is observed at 1000 ^oC and corresponds to the results obtained by Piacentini for the HT sites. The data of the MS show peaks at the same temperatures as for the weight loss as can be observed in Figure 12, indicating that indeed the CO_2 evolves from the catalytic surface at the discussed temperatures Next calculations have been performed to obtain quantitative data of the different $BaCO_3$ species. represents the simulated data from which the relative amounts of LT and HT sites have been calculated. These calculations show that the 30 % of the $BaCO_3$ sites are LT and 70 % are HT.

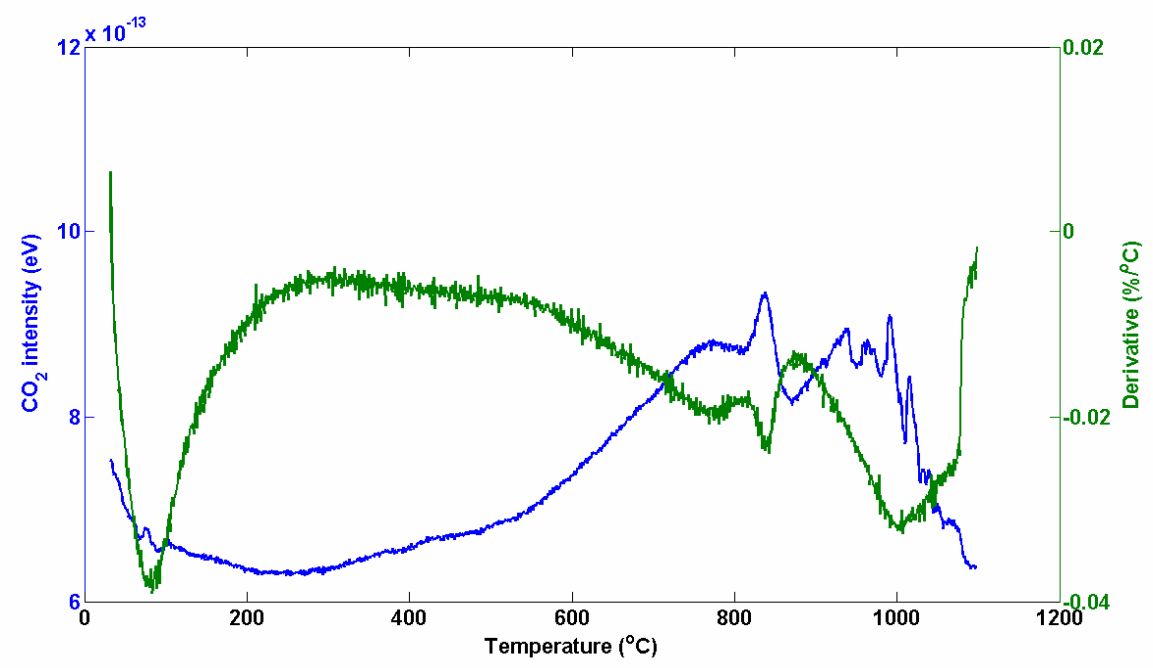

Figure 12: *Results for CO_2 desorption and weight loss. TGA heating rate of 10 ^{o}C/min*

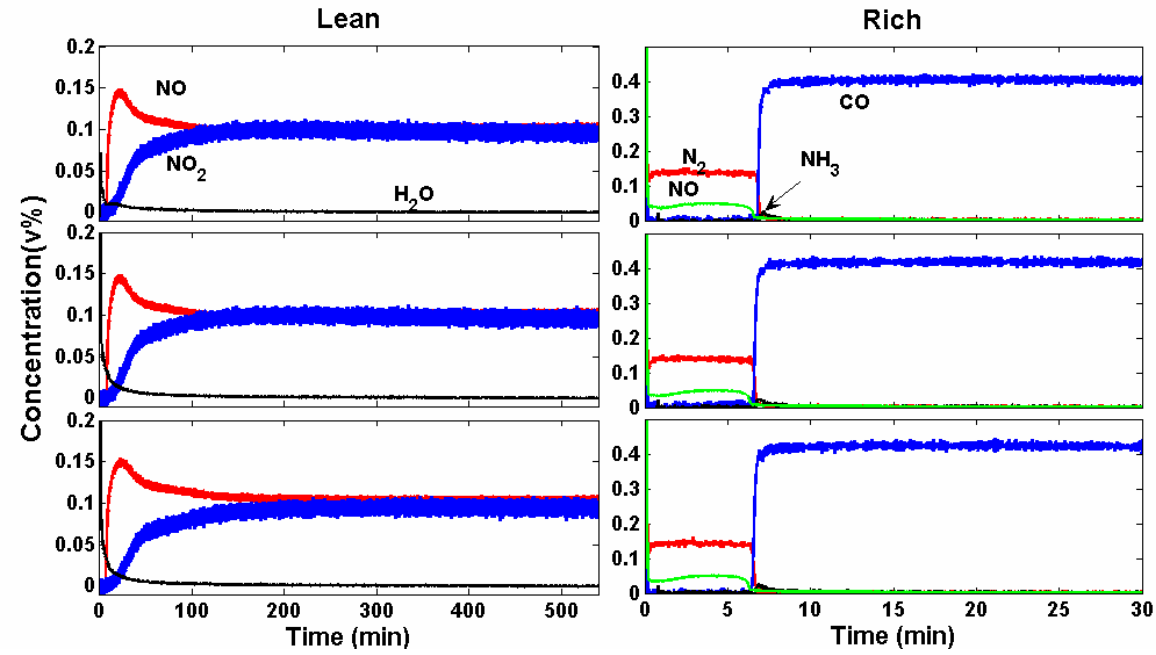

Figure 13: *Experimental results for lean/rich cycling of 9 and 15 hrs respectively for cycles 1, 2 and 3. Performed at T=370^{o}C, lean phase: 0.2 v% NO, 4 v% O_2, 10 v% CO_2, 1 v% Ar. Rich phase: 0.8 v% H_2, 10 v% CO_2, 1 v% Ar. He used as carrier gas.*

5.3. Experiments with CO_2

5.3.1. Activity change

Figure 13 represents the results for the 9/15 hrs. lean/rich cycling experiment performed at 370°C, with the concentration in v% as a function of time in minutes the quantitative results are depicted in Table 9.

Table 9: *Quantitative results for lean/rich cycling of 9 and 15 hrs respectively at T=370°C with CO_2 in lean and rich.*

Cycle nr:	**1**	**2**	**3**
Lean			
Ba% stored	24.9	27.7	27.8
$Ba(OH)_2$ %	9.1	15.8	16.3
Breakthrough time (s)	395	395	385
Rich			
Ba% reduced	23.4	25.1	25.8
Ba% N_2 based	19.4	15.7	16.1
Ba% NO_x based	4	9.3	9.6
Ba% NH_3 based	0.003	0.1	0.1
Reduction efficiency	82.9	62.5	62.5

Cycle nr. 1 shows immediate H_2O formation during lean operation, indicating $Ba(OH)_2$ participation. This participation is 8.8 %. NO breaks through after 390 s. The NO signal shows a maximum after approximately 15 min. NO_2 breaks through after approximately 540 s. $BaCO_3$ also participates in the storage process, because CO_2 formation is observed. However, this is not shown in the figure due to the excess CO_2 present. The total amount of NO_x stored is approximately 25 %. $Ba(OH)_2$ participates for 9.1 % in the NO_x storage.

Switching to the rich phase immediate N_2 formation and NO release are observed. The N_2 production reaches a constant level of 0.14 v% and remains constant for 6.3 min.. The NO release shows an increase towards a plateau. The NH_3 formation is very small, almost zero. CO formation is also observed due to the discussed reversed water gas shift reaction, (Equation 10). CO concentration reaches a level of 0.4 v%. Both CO and NH_3 are observed after N_2 and NO decline. The total amount of reduced $Ba(NO_x)_2$ is 23.4 %, with N_2 formation responsible for 19.4 %, NO release for 4 % and NH_3 almost 0. The reduction efficiency is 82 %.

The second lean phase shows similar results as for the first cycle. However, the amount of NO_x stored is slightly higher and reaches about 28 %. The corresponding rich phase shows no differences compared to the first cycle. Approximately all of the stored NO_x is again released and/or reduced. The N- mass balance is closed within 5 %. The third cycle is a repetition of the second cycle. The NO_x storage is equal in amount and breakthrough timing, again 28 % storage is observed. The NO and NO_2 signal obey NO oxidation behavior at the end of the lean phase. Moreover, the corresponding rich phase shows the same results as well.

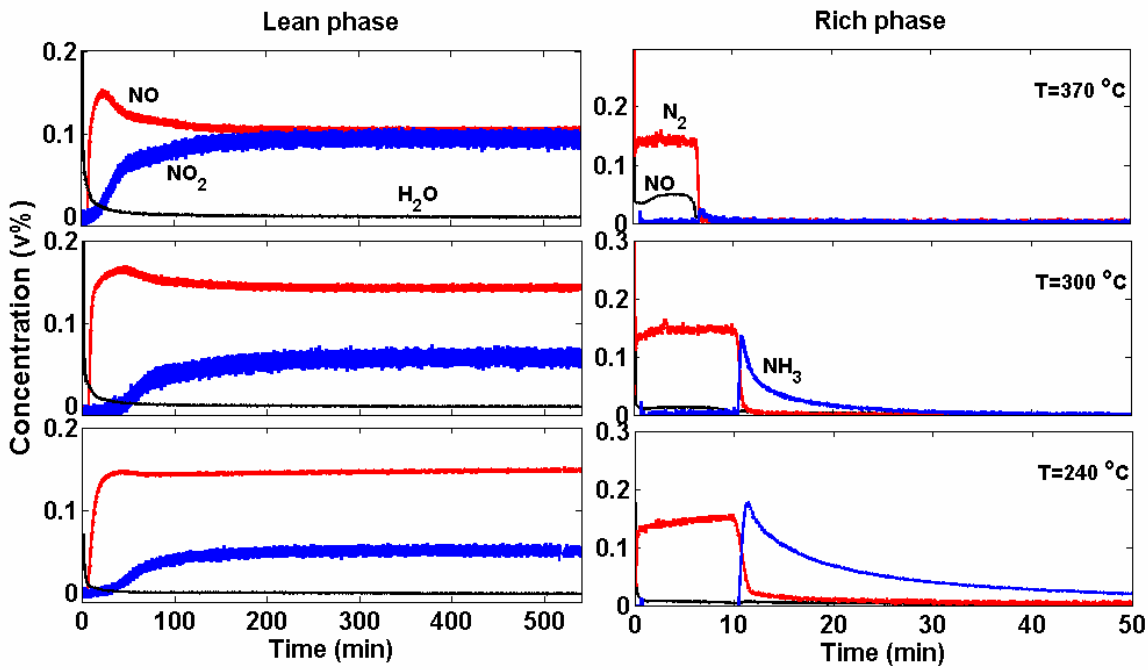

Figure 14: *Lean/rich cycling of 9 and 15 hrs respectively. At: 370, 300 and 240 °C. Lean phase: 0.2 v% NO, 4 v% O_2, 10 v% CO_2 and 1 v% Ar. Rich phase: 0.8 v% H_2, 10 v% CO_2 and 1 v% Ar. He as carrier gas.*

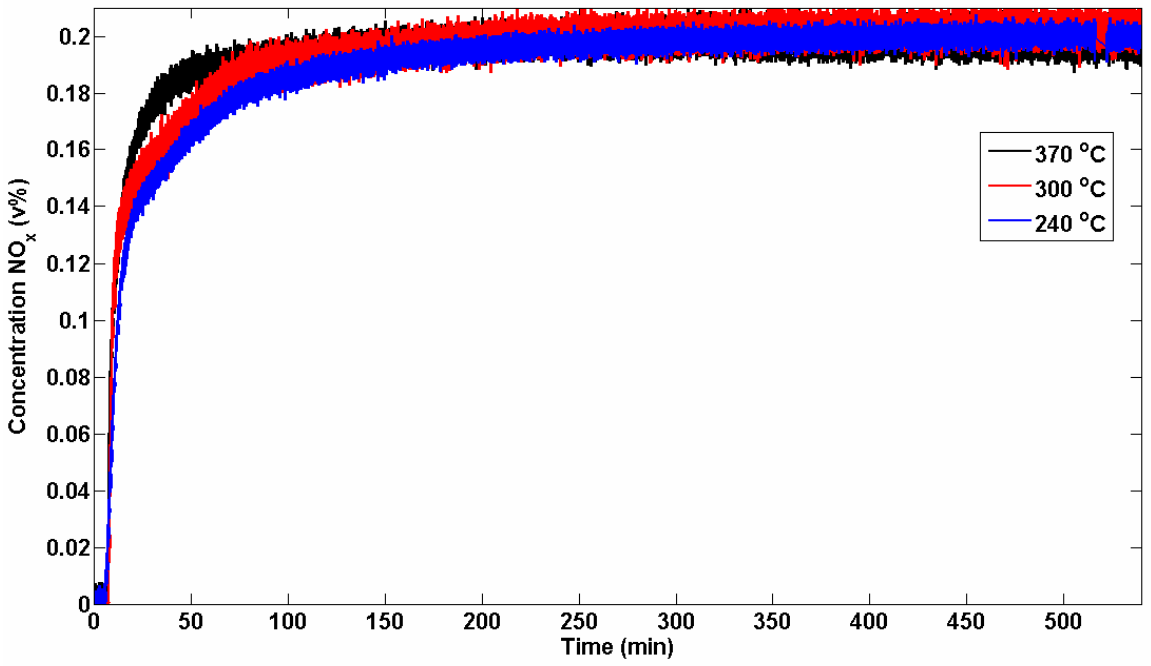

Figure 15: *Lean/rich cycling of 9 and 15 hrs respectively. At: 370, 300 and 240 °C. Lean phase: 0.2 v% NO, 4 v% O_2, 10 v% CO_2 and 1 v% Ar. Rich phase: 0.8 v% H_2, 10 v% CO_2 and 1 v% Ar. He as carrier gas.*

Thus with CO_2 in the feed and at high temperature, about 30% storage is observed and no activity or selectivity change takes place. To support these observations, the physical properties of the catalyst have been measured. The results are depicted in Table 10, where the BET surface area, pore volume and Pt dispersions are depicted. It is shown that the BET surface has barely changed compared to the fresh catalyst. In addition the Pt dispersion has remained the same. The XRD spectrum in Figure 10(B) shows the results for the catalyst after a lean phase. There is no $Ba(NO_3)_2$ observed, while storage has taken place. This implies that almost no bulk sites have participated in the storage process. Therefore, one can state that mainly LT $BaCO_3$ sites have been participating in the storage process. Furthermore, the TGA showed a value of 40 % for the LT $BaCO_3$ sites. With a storage of 30 % it is possible that only LT sites have participated.

Table 10: *BET surface area, pore volume and Pt dispersion*

Conditions	**BET (m^2/g)**	**Pore volume (cm^3/g)**	**Pt – dispersion (%)**
Pretreated catalyst	74	0.22	20
With CO_2 after lean	70	0.23	20
With CO_2 after rich	70	0.22	20

5.2.2. Influence of temperature

For the study on the temperature influence, the cyclic steady states of three different temperatures are observed. The results are depicted in Figure 14 with the concentration in v% as a function of time in min. The quantitative data obtained from these experiments are depicted in Table 11.

Table 11: *Quantitative results at 240, 300 and 370 ^oC. Lean/rich cycling of 9 and 15 hrs respectively.*

Temperature (^oC):	**370**	**300**	**240**
Lean			
Ba% stored	27.8	27.5	29.1
$Ba(OH)_2$ %	16.3	11.3	6.2
Breakthrough time (s)	385	380	250
Rich			
Ba% reduced	25.8	26.9	34.3
Ba% N_2 based	16.1	21.0	20.4
Ba% NO_x based	9.6	2.4	1.2
Ba% NH_3 based	0.1	3.5	12.9
Reduction efficiency	62.5	78 %	59.5 %

When comparing the lean phases, the differences lie in the NO end level and the breakthrough timing. With higher temperature the overshoot in the NO signal becomes higher. The change in steepness of the NO_2 signal can have something to do with $Ba(NO_2)_2$ to $Ba(NO_3)_2$ oxidation (Equation 5). This phenomenon will be elaborated on in section 6. The total NO_x storage for all three temperatures has been depicted in Figure 13. Here, NO_x storage amounts are approximately the same for all three experiments.

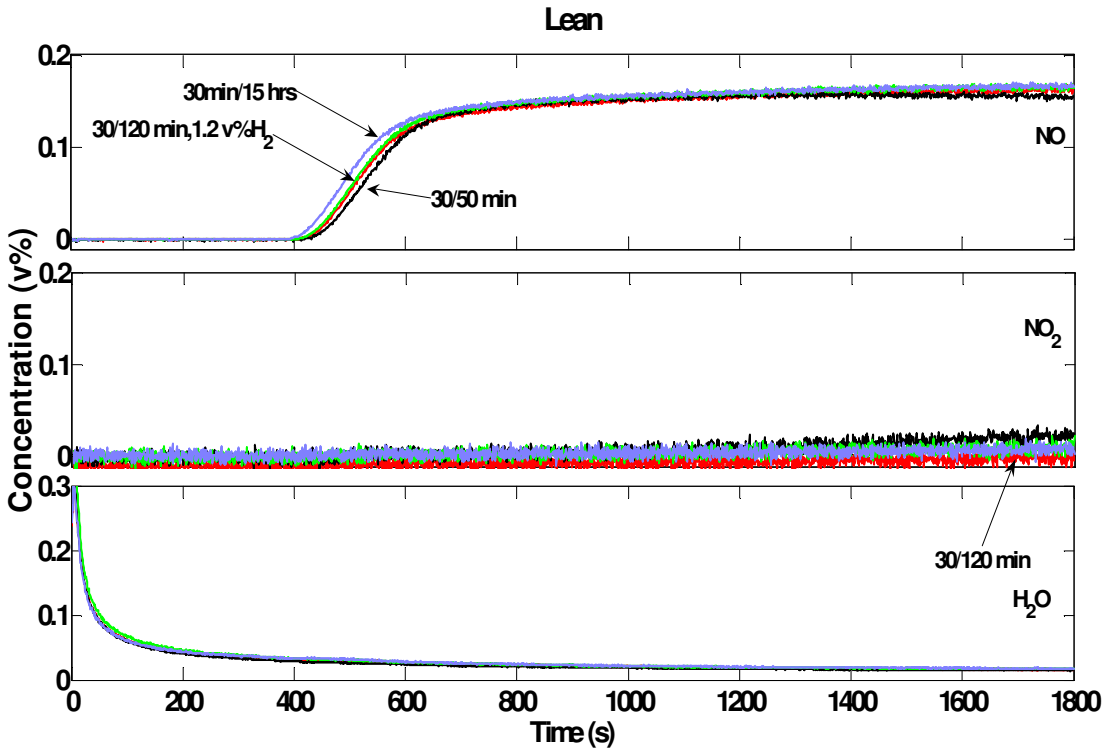

Figure 16A: *Lean operation at 300°C at different rich timing. 30/120 (r), 30/50 (black), 30/120+1.2v%H_2 (g), 30min/15hrs (blue). Lean phase: 0.2 v% NO, 4 v% O_2, 10 v% CO_2 and 1 v% Ar.*

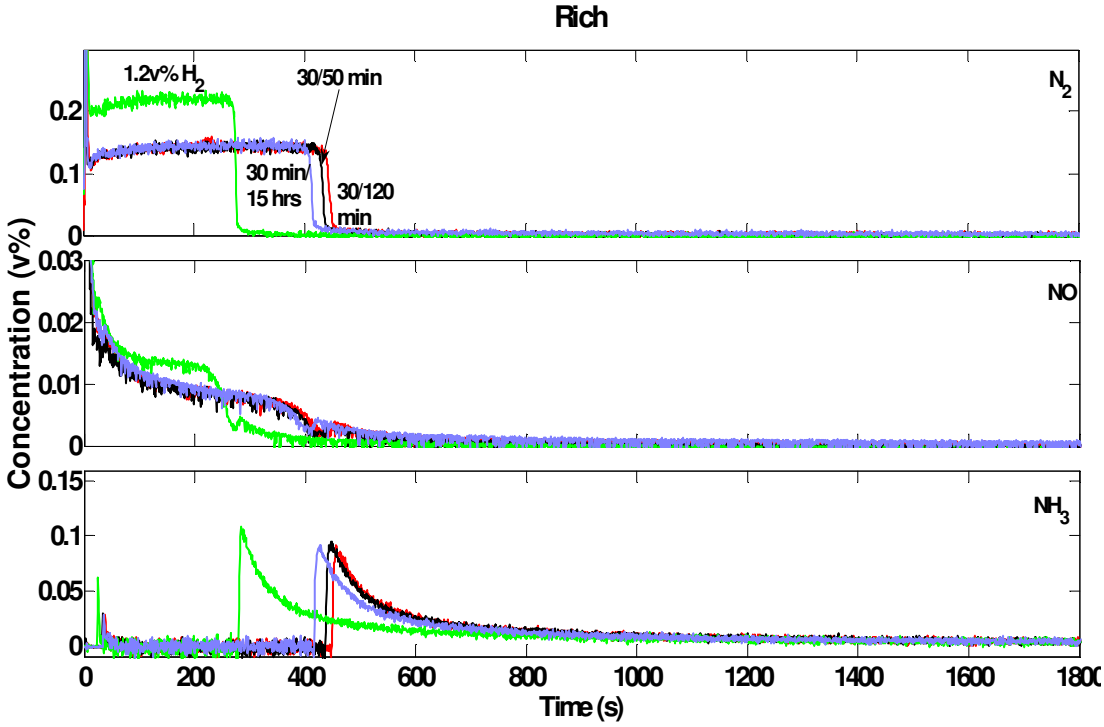

Figure 16B: *Rich operation at 300 °C: 0.8 v% H_2 (and 1.2v%),, 10 v% CO_2 and 1 v% Ar.*

However, the rich phase shows more dissimilarity. The NO desorption at 370°C is much higher than for the lower temperatures. In addition at lower temperatures NH_3 formation is observed with an increase in the amount as the temperature decreases. This is an indication that at lower temperatures the selectivity of the catalyst towards N_2 production goes down, as represented by the reduction efficiency. However, the activity of the catalyst stays the same. Overall one can state that the temperature influences can be found in the way storage and reduction are achieved and not in the amount of NO_x that can be stored. The evidence is provided in Table 11. Furthermore, figure 15 shows NO_x profiles for all three experiments. The surface area above the NO_x signal and below 0.2 v%, which is the inlet concentration, represents the storage. This area is approximately the same for all three experiments. Only the 370 °C shows a small deviation.

5.2.3. Influence of Rich timing

Figure 16 shows the results for the experiments conducted to study the influence of rich timing on the NO_x storage behavior. For this experiment a reference experiment is used with lean/rich cycling of 30 and 120 min respectively. For all experiments the cyclic steady state was reached.

First lean/rich cycling was set at 30/50 minutes. Comparison of the lean phase shows differences in the NO breakthrough time. The total amount of NO_x that is stored corresponds to about 14 %Ba participation. The NO and NO_2 end levels are approximately the same compared to the reference experiment. H_2O is observed from the start indicating $Ba(OH)_2$ participation. The amount is the same for all experiments. The rich phase itself shows a change in N_2 formation time.

Next the lean/rich cycling experiment of 30 and 120 min respectively was started with the rich conditions changed to 1.2v% H_2. Here H_2O formation is observed from the start at a slightly higher level during lean operation. This can be ascribed to the fact that because of the higher H_2 concentration more $Ba(OH)_2$ has been formed during rich operation. NO_x storage has again changed by a decrease in breakthrough time. The total amount stored however, is about 14 %. The rich phase shows a shorter N_2 production time, caused by the higher H_2 concentration; more H_2 means more sites that can react simultaneously. An equal amount of NO_x has been stored but is reduced in a shorter period of time causing the N_2 level to rise. NO desorption and NH_3 formation show the same deviations as were observed with the N_2 signal.

Finally the lean/rich cycling was set at 30 min and 15 hours respectively. Similar results can be expected as for the previous experiment. A long rich phase with a certain amount of H_2 should have the same effect as a short time in which a much larger amount of H_2 is fed. However, this is not the case. H_2O evolves again from the start but the amount that is produced corresponds to the reference experiment. Furthermore, there are no changes in lean behavior except for earlier breakthrough of NO. When we switch to the rich phase, all of the stored NO_x is reduced as was the case with the previous experiments. NO desorption, NH_3 formation and N_2 formation show similar changes compared to the reference experiment as the previous discussed experiments.

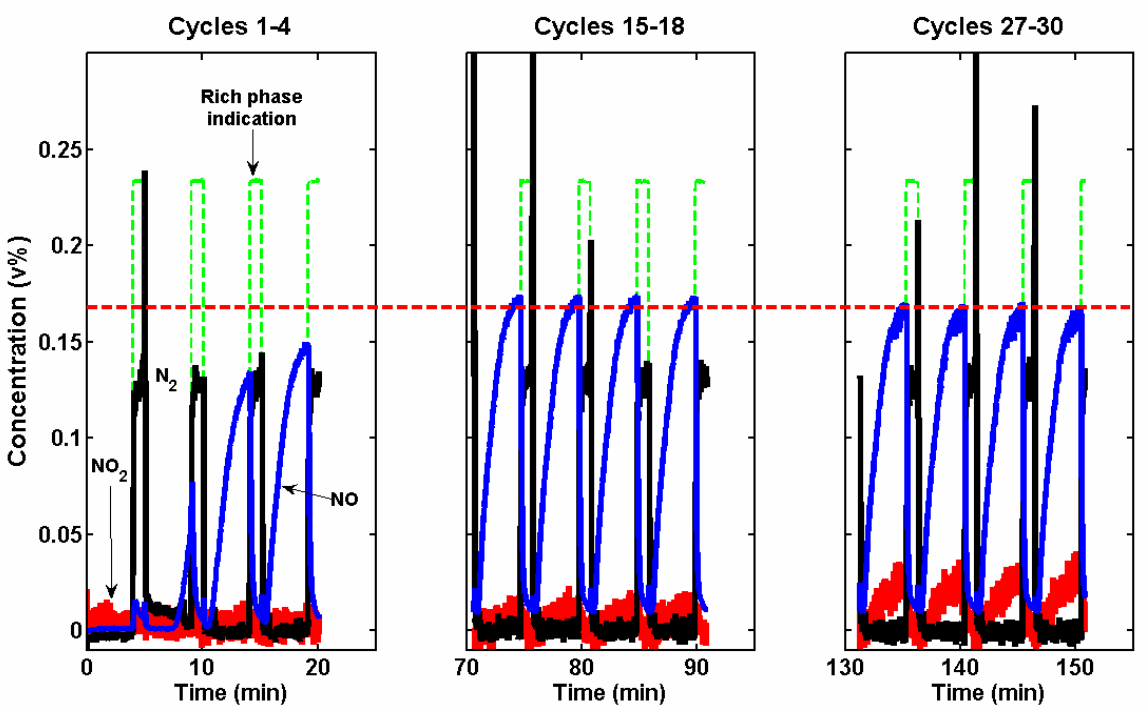

Figure 17: *Transient lean/rich cycling of 4 and 1 min respectively, at T=300 °C. Lean phase: 0.2 v% NO, 4 v% O_2, 10 v% CO_2 and 1 v% Ar. Rich phase: 0.8 v% H_2, 10 v% CO_2 and 1 v% Ar. He was used as carrier gas.*

5.2.4. Transient experiments

With lean/rich cycling of 4 and 1 min respectively, we can approach real life application. The results for this experiment are shown in Figure 15, with the concentration in v% as a function of time in minutes.

Observing cycles 1-4, one can see that during the first cycle, complete NO_x storage is obtained. During the following rich phase, immediate N_2 production is observed, at a level of 0.13 v%. One minute rich time is too short to release/reduce all of the stored NO_x. This leads to an accumulation of $Ba(NO_3)_2$. Furthermore there is no NH_3 formation. Cycle nr. 2 shows NO breakthrough at the end of the 4 min lean phase, NO_2 still shows no breakthrough which is in correspondence with the results for longer switching times. Because there NO_2 was breaking through later than NO, as is happening with this experiment. The rich phase shows again immediate N_2 formation with a small increase in concentration. The following cycles show similar behavior, apart from the NO which breaks through earlier.

Next cycles 15-18 are plotted. The NO breakthrough time has reached a steady point. The concentration at the end of the lean phase has reached a higher level. Furthermore NO_2 has started to break through during the lean phase. The N_2 levels in the rich phases are approximately of the same level. Observing cycle nr. 27-30, a decrease in NO end level is observed. For the experiments performed at lean/rich cycling of 9and 15 hrs respectively, a maximum for NO was observed. The red dotted line shows that the NO level also reaches a maximum in this short switching experiment. Overall it is shown that the characteristics of the long switching experiments are observed in the short switching experiments as well, i.e. a maximum for NO, NO_2 breakthrough later than NO and immediate N_2 production.

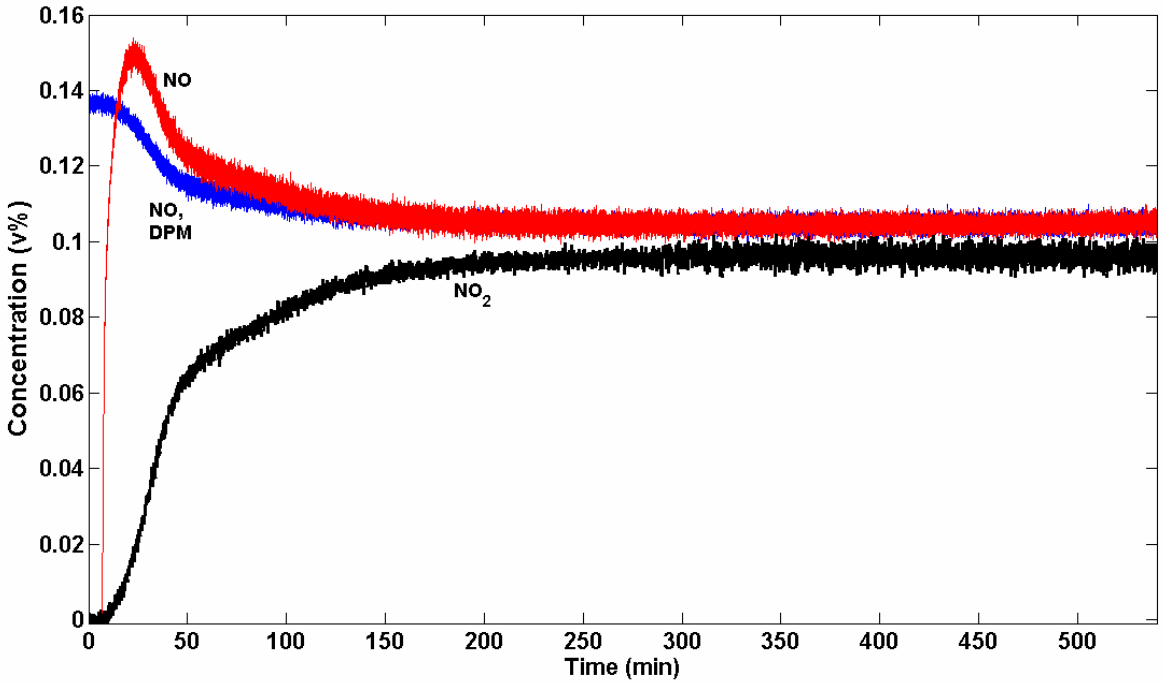

Figure 18: *Lean profile for NO and NO_2, performed at 370 ^oC, 9 hrs. With 0.2 v% NO, 4 v% O_2, 10 v% CO_2, 1 v% Ar. The blue line represents NO concentration in case of DPM.*

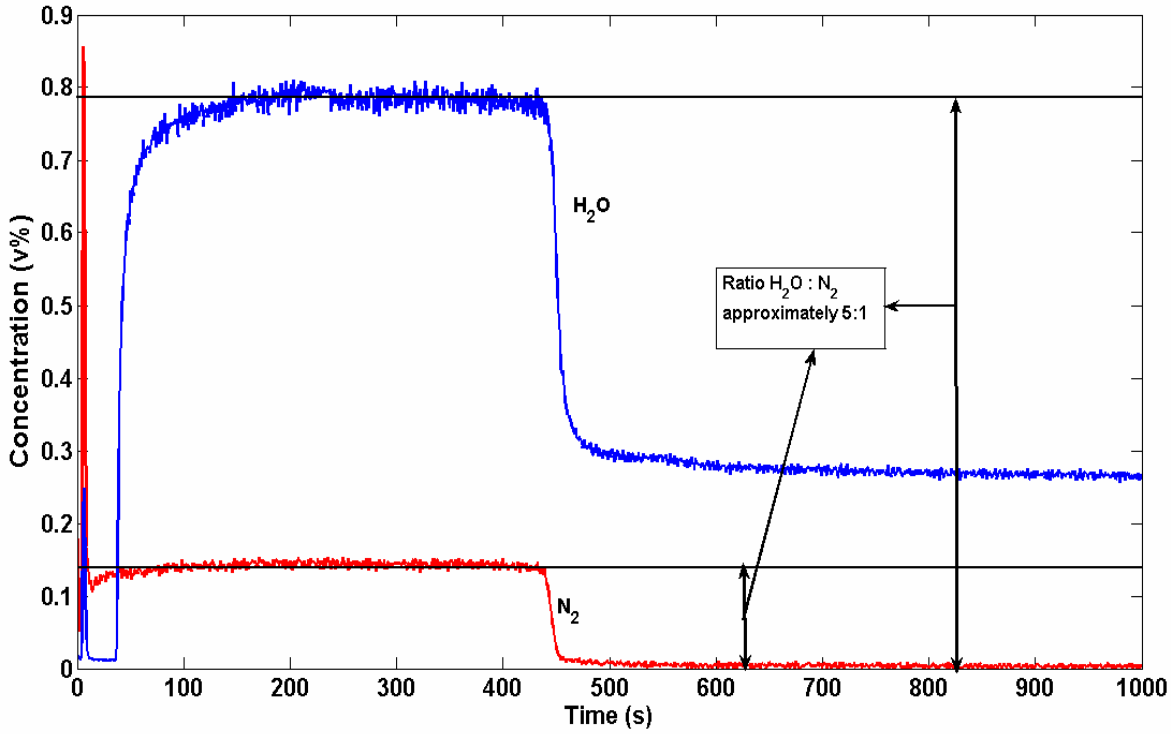

Figure 19: *Ratio H_2O : N_2 in the rich phase with 0.8 v% H_2, 10 v% CO_2 and 1 v% Ar. He was used as carrier gas.*

6. Discussion

6.1. Lean characteristics.

As mentioned in section 3.2, several routes can be distinguished towards NO_x storage. The generally most used is the disproportionation mechanism (DPM) [4,5,12], resulting in storage through NO_2 only. If it is considered that during the discussed experiments, only the DPM is taking place, a calculation can be made what the amount of NO should be. Consider the experiment at 370 ^oC with lean/rich cycling of 9 and 15 hrs respectively. The lean phase is depicted in Figure 18. The NO oxidation (Equation 1) precedes the DPM and is assumed to set in rapidly. Furthermore, at the end of the 9 hrs lean phase, the storage has "stopped" and only the NO oxidation takes place. The concentrations for NO and NO_2 observed there would be observed throughout the 9 hrs lean phase, if NO oxidation was the only reaction taking place. The DPM is described in Equation 2 and shows for 3 moles of NO_2 stored, 1 mole of NO is formed. The blue line in Figure 17 shows the result for 9 hrs lean operation with only DPM occurring. The NO concentration is calculated with the mentioned assumptions as follows:

$$NO_{DPM} = C_{NO,ox} + ((C_{NO_2,ox} - C_{NO_2}(t))/3) \qquad \text{(Eq. 11)}$$

As can be observed in Figure 17, the NO concentrations of the DPM case and the experimental results differ. After all, no dead time for NO is observed when DPM takes place. This shows that DPM is not the only mechanism that is involved in the NO_x storage. However, the DPM can be responsible for early sorption times. This is described by Epling et al. [12]. They state that it is possible for released NO to be captured downstream in the reactor bed to be oxidized to NO_2 and subsequently be stored. Moreover, NO_2 can also be stored directly without the formation of NO into $Ba(NO_3)_2$ as described in Equation 3. This can then explain why no NO is observed during storage of NO_2. Another eligible explanation for the dead time of NO, is the nitrite route (Equation 4) by which NO is stored directly on Ba sites to form $Ba(NO_2)_2$. This leads to another observation made in previous sections, that a maximum in the NO signal can be detected. With the nitrite route, per mole $Ba(NO_2)_2$ oxidized to $Ba(NO_3)_2$, 2 mole NO is formed. The maximum in the NO signal (Figure 18) corresponds to a gradient change in the NO_2 signal. During the maximum, the NO_2 breaks through quite rapidly, implying less NO_2 is used for storage. This is an indication that $Ba(NO_2)_2$ have been oxidized to $Ba(NO_3)_2$.

6.2. Rich characteristics

In the results different components have been discussed during rich operation. In addition H_2O and O_2 can be examined. H_2O, O_2 have in common that they show a dead time or very low value during the first 30-50 seconds of the rich operation. If we look at the release mechanism more closely, we can describe it as depicted in Equations 13 to 16.

$$Ba(NO_3)_2 + H_2 + CO_2 \rightarrow BaCO_3 + 2\,NO + O_2 + H_2O \qquad \text{(R-eq. 12)}$$

$$Ba(NO_3)_2 + H_2 + CO_2 \rightarrow BaCO_3 + 2\,NO_2 + H_2O \qquad \text{(R-eq. 13)}$$

$$Ba(NO_2)_2 + H_2 + CO_2 \rightarrow BaCO_3 + 2\,NO + H_2O \qquad \text{(R-eq. 14)}$$

$$2\,NO + 2\,H_2 \xrightarrow{Pt} N_2 + 2\,H_2O \qquad \text{(R-eq. 15)}$$

$$2\,NO_2 + 2\,H_2 \xrightarrow{Pt} N_2 + 2\,H_2O + O_2 \qquad \text{(R-eq. 16)}$$

During the first 30 to 50 s, O_2 and H_2O show a dead time. After this period, O_2 and H_2O increase to a constant value of 0.02 v% and 0.8 v% respectively. The delay in H_2O evolution can be due to adsorption on Ba sites resulting in $Ba(OH)_2$. Lietti et al. [5] described this phenomenon. They describe that the 50 s dead time corresponded to desorption of CO_2, in which case $BaCO_3$ is exchanged for $Ba(OH)_2$. Furthermore, it is possible for H_2O to adsorb on γ-Al_2O_3. The delay in O_2 evolution can be explained with adsorption of O_2 on Pt sites. If O_2 is assumed to evolve from the start with a constant value of 0.02 v%, calculations can be made on the amount of Pt sites involved. Furthermore the assumption is made that O_2 is bridged on two Pt sites. The Pt dispersion must also be taken into account to perform calculations on the available Pt sites. The calculation is depicted in Appendix 3. The Pt participation is about 40 %. Apparently this leaves enough sites to perform reduction of NO_2 ad NO to N_2. However, for a short period of time.

In the rich phase evidence on what species are formed ultimately in the lean phase, $Ba(NO_2)_2$ or $Ba(NO_3)_2$, can be found. If we consider the overall reaction towards N_2 production from nitrates then for each mole of N_2 produced, 5 moles of H_2O are produced (R-eq. 15).

$$Ba(NO_3)_2 + 5\,H_2 + CO_2 \xrightarrow{Pt} BaCO_3 + N_2 + 5\,H_2O \qquad \text{(R-eq. 15)}$$

$$Ba(NO_2)_2 + 3\,H_2 + CO_2 \xrightarrow{Pt} BaCO_3 + N_2 + 3\,H_2O \qquad \text{(R-eq. 16)}$$

If we consider nitrite release/reduction, the mole ratio of N_2:H_2O is 1:3. In figure 18 the N_2 and H_2O concentrations in v% are plotted as a function of time (s). The figure shows a N_2/H_2O ratio 1:5. This is in correspondence with nitrate release/reduction. Therefore, we can state that at the end of the lean phase the catalyst overall consists of $Ba(NO_3)_2$.

Finally there have been observations during rich operation of NH_3 (Equation 8) and CO formation (Equation 10). The production of these components takes place after N_2 production and NO desorption have declined. For the formation of NH_3 $Ba(NO_3)_2$ or $Ba(NO_2)_2$ is necessary as N donor. The N_2 production and NO release are faster reactions than NH_3 formation [7]. This can explain why NH_3 formation starts when N_2 and NO concentrations have declined. For CO, the reason for delay in evolution is that the amount of H_2 fed is completely used for reduction of $Ba(NO_3)_2$ into N_2 and release of NO.

7. Conclusions and recommendations

The activity change experiments without CO_2 lead to the following conclusions:

- Activity change can be observed even at short lean/rich cycling times in the order of minutes.
- Selectivity change can be observed.
- BET and Pt-dispersion showed changes of about 40 % decrease.
- HT sites participate in the storage process.

Experimentation with CO_2 in the feed showed the following:

- No activity change is observed even after lean/rich cycling of 9 and 15 hrs respectively.
- The BET and Pt dispersion did not change compared to a fresh catalyst.
- XRD showed $BaCO_3$ sites, indicating no HT sites participation in the storage process. With TGA measurements indicating 40 % of Ba present as LT sites, the Ba utilization of 30 % is possible without the participation of HT sites.
- Temperature has influence on the NO_x storage behavior. Breakthrough profiles are different. However, the total amount NO_x stored seems temperature independent.
- Higher temperature leads to higher NO desorption values. NO desorption is observe from the start of the rich phase.
- Longer rich timing leads to a decrease in NO breakthrough time. This also holds for the N_2 production time.
- Transient experiments show similar results compared to long cycling experiments: For NO breakthrough a maximum is observed, NO_2 shows a delay compared to NO.

The discussion has shown that:

- The DPM is not the only mechanism taking place during storage.
- Stored nitrites have been oxidized to nitrates.
- After lean operation mostly $Ba(NO_3)_2$ has been formed.
- Storage of O_2 on Pt sites during rich phase operation, does not influence the release and reduction of $Ba(NO_3)_2$.

Overall, extensive modeling is necessary to make sure that the stated pathways towards NO_x storage are correct. When a proper model is constructed it should then converge with the measured data. Furthermore, when the experiments must come a step closer to real life application, the incorporation of H_2O is a possibility. Some research has already been done on this subject and often in combination with CO_2.

Appendix 1: References

[1] S. Matsumoto, CATTECH 4,2 (2000) 102-109
[2] H. Mahzoul, J.F. Brilhac, P. Gilot, Applied Catalysis B: Environmental 20 (1999) 47-55
[3] E. Fridell, H. Persson, B. Westerberg, L. Olsson, M. Skoglundh, Catalysis Letters 66 (2000) 71-74
[4] N.W. Cant, M.J. Patterson, Catalysis Today 73 (2002) 271-278
[5] L. Lietti, P. Forzatti, I. Nova, E. Tronconi, Journal of Catalysis 204, 175-191 (2001)
[6] I. Nova, L. Castoldi, L. Lietti, E. Tronconi, P. Forzatti, Catalysis Today 75 (2002) 431-437
[7] L. Castoldi, I. Nova, L. Lietti, P.Forzatti, Catalysis today 96 (2004) 43-52
[8] L. Olsson, E. Fridell, M. Skoglundh, B. Andersson, Catalysis Today 73 (2002) 263-270
[10] M. Piacentini, M. Maciejewski, A. Baiker, Applied Catalysis B: environmental 59 (2005) 197-195
[11] M.Piacentini, M. Maciejewski, A. Baiker, Applied Catalysis B: Environmental 60 (2005) 273-283
[12] W.S. Epling, J.E. Parks, G.C. Campbell, A. Yezerets, N.W. Currier, L.E. Campbell, Catalysis Today 96 (2004) 21-30
[13] C.M.L. Scholz, V.R. Gangwal, J.H.B.J. Hoebink, J.C. Schouten, Applied Catalysis B: Environmental
[14] S. Balcon, C. Potvin, L. Salin, J.F. Tempère, G. Djéga-Mariadassou, Catalysis Letters 60 (1999) 39-43
[15] W.S. Epling, G.C. Campbell, J.E. Parks, Catalysis Letters Volume 90, Nos. 1-2, September 2003
[16] I. Nova, L. Castoldi, F. Prinetto, V. Dal Santo, L. Lietti, E. Tronconi, P. Forzatti, G. Ghiotti, R. Psaro, S. Recchia, Topics in Catalysis 30/31, July 2004
[17] L. Olsson, H. Persson, E. Fridell, M. Skoglundh, B. Andersson, Journal of Physical Chemistry B 2001, 105, 6895-6906
[18] L. Olsson, B. Westerberg, H. Persson, E. Fridell, M. Skoglundh, B. Andersson, Journal of Physical Chemistry B, 103, 10433-10439
[19] X. Chen, J. Schwank, J. Li, W.F. Schneider, C.T. Goralski Jr, P.J. Schmitz, Applied Catalysis B: Environmental 61 (2005) 189-200
[20] A. Amberntsson, H. Persson, P.Engström, B. Kasemo, Applied Catalysis B: Environmental 31 (2001) 27-38
[21] J. I. Theis, U. Göbel, M. Kögel, T. P. Kreuzer, D. Lindner, E. Lox, L. Ruwisch, SAE Technical paper series, 2002-01-0057
[22] F. Rodrigues, L.Juste, C. Potvin, J.F. Tempère, G. Blanchard and G. Djèga-Mariadassou, Catalysis Letters Volume 72, No. 1-2, 2001

Appendix 2: Argon correction

In order to compensate for intensity loss of the MS, the Argon signal was fixed to an intensity of 1.42e-9 for 1 v% of Ar in the feed. The other m/e's were corrected for this value according to the following equation:

$$\mathrm{Int(X)}_{\mathrm{cor}} = \frac{\mathrm{IntAr(fix)}}{\mathrm{IntAr(MS)}} * \mathrm{IntX(MS)}$$

IntAr(fix) = fixed Ar intensity of 1.42e-9
IntAr(MS) = Ar intensity at t = t
IntX(MS) = intensity component X at t = t

Appendix 3

Calculation for Pt participation in possible O_2 storage.

$$C_{Pt} = \frac{w_{Pt} * m_{cat}}{M_{Pt}} * Disp_{Pt}$$

$$C_{O_2} = \frac{c_{O_2} * t * f}{100\,\%}$$

$$\text{Pt participation} = \frac{C_{O_2} * 2}{C_{Pt} * m_{cat}} * 100$$

C_{Pt}	= mole Pt	
C_{O2}	= concentration O_2 stored in moles	
w_{Pt}	= weight fraction Pt	= 0.01
m_{cat}	= catalyst weight in gram	= 1.9386 g
M_{Pt}	= molar weight of Pt in mole/gram	= 195.08 g/mole
$Disp_{Pt}$	= Pt dispersion	= 0.2
t	= dead time of O_2	= 30 s
f	= molar feed	= $7.43e^{-4}$ mole/s